Supplementary Materials for

Harnessing electro-generated excitons for tunable lanthanide nanocrystal electroluminescence

This file includes:

Materials and Methods

Materials and Instruments

All reagents and solvents used for the synthesis of the compounds were purchased from Aldrich and Acros companies and used without further purification. ^{1}H NMR spectra were recorded using a Varian Mercury plus 400NB spectrometer, with tetramethylsilane (TMS) as the internal standard. Molecular masses were determined using a FINNIGAN LCQ Electro-Spraying Ionization-Mass Spectrometer (ESI-MS) or a MALDI-TOF mass spectrometer. Elemental analyses were performed using a Vario EL III elemental analyzer. Suitable single crystals for X-ray diffraction (XRD) analysis were obtained by slowly diffusing 12 mL of *n*-hexane into a 3 mL dichloromethane solution of ArPPOA (10 mg) at room temperature. XRD data were collected at 295 K on a Rigaku Xcalibur E diffractometer with graphite-monochromatized Mo Kα radiation (λ = 0.71073 Å) in ω scan mode. The structures were solved using direct methods and difference Fourier syntheses. Non-hydrogen atoms were refined by full-matrix least-squares techniques on F2 with anisotropic thermal parameters. Hydrogen atoms attached to carbons were placed at calculated positions (C−H = 0.93 Å) with U(H) = 1.2Ueq(C), following the riding model approximation. All calculations were carried out using the SHELXL97 program.

Transmission electron microscopy (TEM) measurements were performed using a field-emission transmission electron microscope (JEOL-JEM 2010F) operated at an acceleration voltage of 200 kV. Absorption and photoluminescence (PL) emission spectra were measured using a SHIMADZU UV-3150 spectrophotometer and a SHIMADZU RF-5301PC spectrophotometer, respectively. Cyclic voltammetry (CV) was conducted using an Eco Chemie B. V. AUTOLAB potentiostat in a three-electrode cell with a glassy carbon working electrode, a platinum wire counter electrode, and a silver/silver chloride (Ag/AgCl) reference electrode. Electrochemical experiments were carried out under a nitrogen atmosphere at room temperature in dichloromethane. Phosphorescence spectra were measured in ethanol using an Edinburgh FPLS 1000 fluorescence spectrophotometer at 77 K, with cooling provided by liquid nitrogen.

Time decay spectra was measured using the time-correlated single photon counting (TCSPC) method with a picosecond hydrogen lamp for the 100 ps-10 μs range and a microsecond pulsed Xenon light source for 1 μs-10 s lifetime measurements. The synchronization photomultiplier collected the signal and the Multi-Channel Scaling Mode of the PCS900 fast counter PC plug-in card was used for data processing. Prompt and delayed fluorescence lifetimes were respectively measured with nanosecond and microsecond time decay methods. Lifetime values were simulated using an exponential fitting function in Fluoracle software.

Nanoparticle-based films (20-40 nm) for optical analysis were prepared through spin coating. Photoluminescence quantum yields (PLQY) of these films were measured through a labsphere 1-M-2 integrating sphere (ϕ = 6") coated by Benflect, providing efficient light reflection across a wide range of 200-1600 nm. The integrating sphere was coupled with the FPLS 1000 system. The absolute PLQY was determined by recording two spectral (emission) scans. The first spectrum captured both the scattered light and the emission from the sample, while the second spectrum measured the scattered light from the Benflect coating. By integrating and subtracting the scattered light parts from both spectra, the photon number absorbed by the sample (N_a) was determined. The emission of the sample was integrated to calculate the emissive photon number (N_e). The absolute PLQY (η) was then calculated using the equation of $\eta = N_e/N_a$. Spectral correction (emission arm) was applied to the raw data after background subtraction, and the quantum yield was calculated from the spectrally corrected curves using the F900 software wizard.

Synthesis Details

Diphenyl(*o*-tolyl)phosphine oxide (TPPOM): Under an argon atmosphere, 1-bromo-2-methylbenzene (1.186 mL, 10 mmol) in 10 mL of dry ether was added dropwise to a mixture of magnesium turnings (0.267 g, 11 mmol) and a small piece of iodine in 10 mL of dry ether at room temperature. The reaction was stirred at 40 °C for one hour. After cooling to 0 °C, chlorodiphenylphosphine (1.980 mL, 11 mmol) in 10 mL of dry ether was added dropwise and stirred for 12 h. The reaction was quenched by adding water, and the mixture was extracted with CH_2Cl_2 (3 × 30 mL). The CH_2Cl_2 solution was concentrated to 30 mL, then 30% H_2O_2 (4.5 mL, 40 mmol) was added at 0 °C and stirred for four hours. After another extraction with CH_2Cl_2 (3 × 30 mL), .the organic phase was combined and dried with anhydrous Na_2SO_4. The solvent was removed *in vacuo*. The product was purified by flash column chromatography, affording 2.6 g of white powder in 90% yield. ^{1}H NMR (TMS, $CDCl_3$, 400 MHz): δ = 7.708-7.612 (m, 4H), 7.591-7.519 (m, 2H), 7.515-7.390 (m, 5H), 7.319-7.270 (m, 1H), 7.115 (t, J = 7.2 Hz, 1H), 6.998 (q, J_1 = 13.6 Hz, J_2 = 7.2 Hz, 1H), 2.453 ppm (s, 3H). LDI-TOF: m/z (%): 292.10 (100) [M^+]; elemental analysis (%) for $C_{19}H_{17}OP$: C 78.07, H 5.86, O 5.47; found: C 78.09, H 5.89, O 5.50.

(4-Bromo-2-methylphenyl)diphenylphosphine oxide (TPPOMBr): The synthetic procedure was similar to that of TPPOM, except for using 4-bromo-1-iodo-2-methylbenzene (2.959 g, 10 mmol) instead of 1-bromo-2-methylbenzene. The product yielded 3.3 g of white powder (90% yield). ^{1}H NMR (TMS, DMSO-d_6, 400 MHz): δ = 7.680-7.605 (m, 3H), 7.604-7.525 (m, 8H), 7.489 (d, J = 8.0 Hz, 1H), 6.857 (q, J_1 = 13.2 Hz, J_2 = 8.4 Hz, 1H), 2.288 ppm (s, 3H). LDI-TOF: m/z (%): 370.01 (100) [M^+]; elemental analysis (%) for $C_{19}H_{16}BrOP$: C 61.48, H 4.34, O 4.31; found: C 61.50, H 4.36, O 4.35.

(4-(9H-carbazol-9-yl)-2-methylphenyl)diphenylphosphine oxide (CzPPOM): Under an argon atmosphere, TPPOMBr (1.856 g, 5 mmol), carbazole (2.508 g, 15 mmol), CuI (0.095 g, 0.5 mmol) and K_2CO_3 (2.073 g, 15 mmol) were dissolved in 50 mL of 1,3-dimethyl-2-imidazolidinone (DMI) and heated to 190 °C for 12 h. After cooling to room temperature, the mixture was poured into water and extracted with dichloromethane (3 × 10 mL) again. The organic layers were combined and dried with anhydrous Na_2SO_4, and the solvent was removed *in vacuo*. The crude product was purified by column chromatography, affording 1.8 g of white powder (80% yield). ^{1}H NMR (TMS, DMSO-d_6, 400 MHz): δ = 8.231 (d, J = 7.6 Hz, 2H), 7.753-7.694 (m, 3H), 7.693-7.643 (m, 4H), 7.644-7.577 (m, 4H), 7.542 (d, J = 8.0 Hz, 1H), 7.497 (d, J = 8.0 Hz, 2H), 7.411 (t, J = 7.6 Hz, 2H), 7.279 (t, J = 7.2 Hz, 2H), 7.209 (q, J_1 = 13.6 Hz, J_2 = 8.4 Hz, 1H), 2.432 ppm (s, 3H). LDI-TOF: m/z (%): 457.16 (100) [M^+]; elemental analysis (%) for $C_{31}H_{24}NOP$: C 81.38, H 5.29, N 3.06, O 3.50; found: C 81.39, H 5.30, N 3.08, O 3.54.

(4-(3,6-Di-*tert*-butyl-9H-carbazol-9-yl)-2-methylphenyl)diphenylphosphine oxide (tBCzPPOM): The synthetic procedure was similar to that of CzPPOM, except for using 3,6-di-*tert*-butyl-carbazole (4.188 g, 15 mmol) instead of carbazole. The yield was 2.2 g of white powder (80% yield). ^{1}H NMR (TMS, $CDCl_3$, 400 MHz): δ = 8.138 (s, 2H), 7.711 (q, J_1 = 11.6 Hz, J_2 = 7.6 Hz, 4H), 7.480 (s, 1H), 7448-7.332 (m, 10H), 7.299 (d, J = 8.0 Hz, 1H), 7.220 (q, J_1 = 13.2 Hz, J_2 = 8.0 Hz, 1H), 2.515 (s, 3H), 1.385 ppm (s, 18H). LDI-TOF: m/z (%): 569.28 (100) [M^+]; elemental analysis (%) for $C_{39}H_{40}NOP$: C 82.22, H 7.08, N 2.46, O 2.81; found: C 82.25, H 7.07, N 2.50, O 2.83.

(4-(9,9-Dimethylacridin-10(9H)-yl)-2-methylphenyl)diphenylphosphine oxide (DMACPPOM): In an argon atmosphere, *tris*(dibenzylideneacetone)dipalladium (0.366 g, 0.4 mmol) and (*t*-Bu)$_3$P (0.094 mL, 0.4 mmol) were mixed in toluene (10 mL) and stirred for 20 min at room temperature. TPPOMBr (3.700 g, 10 mmol), 9,9-dimethyl-9,10-dihydroacridine (DMAC, 2.509 g, 12 mmol), *t*-BuONa (1.922 g, 20 mmol) were added, and the mixture was heated to 90 °C and stirred for six hours. After the reaction, the toluene solvent was removed by distillation, and the solid was dissolved in dichloromethane. The crude product was purified by flash column chromatography, yielding 3.9 g of pale yellow powder (80% yield). ^{1}H NMR (TMS, $CDCl_3$, 400 MHz): δ = 7.739 (q, J_1 = 12.0 Hz, J_2 = 6.8 Hz, 4H), 7.581 (t, J = 7.2 Hz, 2H), 7.570-7.499 (m, 4H), 7.438 (dd, J_1 = 7.6 Hz, J_2 = 1.2 Hz, 2H), 7.305-7.267 (m, 1H), 7.268-7.215 (m, 1H), 7.120 (d, J = 8.0 Hz, 1H), 6.978 (t, J = 7.2 Hz, 2H), 6.920 (t, J = 7.2 Hz, 2H), 6.266 (d, J = 8.0 Hz, 2H), 2.519 (s, 3H), 1.667 ppm (s, 6H). LDI-TOF: m/z (%): 499.21 (100) [M^+]; elemental analysis (%) for $C_{34}H_{30}NOP$: C 81.74, H 6.05, N 2.80, O 3.20; found: C 81.75, H 6.06, N 2.84, O 3.22.

(4-(9,9-Diphenylacridin-10(9H)-yl)-2-methylphenyl)diphenylphosphine oxide (DPACPPOM): The synthetic procedure was similar to that of DMACPPOM, except for using 9,9-diphenyl-9,10-dihydroacridine (DPAC, 3.998 g, 12 mmol) instead of DMAC. The reaction yielded 4.9 g of white powder with an 80% yield. ^{1}H

NMR (TMS, $CDCl_3$, 400 MHz): δ = 7.689 (q, J_1 = 12.0 Hz, J_2 = 7.2 Hz, 4H), 7.567 (t, J = 7.2 Hz, 2H), 7.550-7.464 (m, 4H), 7.291-7.193 (m, 6H), 7.126 (q, J_1 = 13.6 Hz, J_2 = 8.0 Hz, 1H), 7.112-7.039 (m, 2H), 7.004-6.927 (m, 5H), 6.922-6.843 (m, 5H), 6.425 (d, J = 8.0 Hz, 2H), 2.444 ppm (s, 3H). LDI-TOF: m/z (%): 623.24 (100) [M^+]; elemental analysis (%) for $C_{44}H_{34}NOP$: C 84.73, H 5.49, N 2.25, O 2.57; found: C 84.74, H 5.51, N 2.28, O 2.60.

2-(Diphenylphosphoryl)benzoic acid (TPPOA): Powdered $KMnO_4$ (3.161 g, 20 mmol) was added in four portions over 1.5 h to a boiling mixture of diphenyl(*o*-tolyl)phosphine oxide (TPPOM) (1.461 g, 5 mmol), pyridine (25 mL), and water (10 mL), maintaining gentle boiling throughout. The mixture was boiled for 5 h, after which pyridine and water were removed by distillation. Upon cooling to room temperature, 1 mL (6 mmol/mL) of hydrochloric acid in 10 mL of H_2O was added dropwise and stirred for 30 min. The mixture was extracted with water and chloroform (3 × 10 mL). The organic layers were combined and dried with anhydrous Na_2SO_4. The solvent was removed *in vacuo*. The crude product was purified by column chromatography, yielding 1.1 g of white powder with a yield of 70%. ^{1}H NMR (TMS, DMSO-d_6, 400 MHz): δ = 13.086 (s, 1H), 7.904-7.845 (m, 1H), 7.701 (t, J = 7.6 Hz, 1H), 7.628 (t, J = 7.6 Hz, 1H), 7.610-7.539 (m, 5H), 7.539-7.455 ppm (m, 6H). LDI-TOF: m/z (%): 322.08 (100) [M^+]; elemental analysis (%) for $C_{19}H_{15}O_3P$: C 70.81, H 4.69, O 14.89; found: C 70.83, H 4.69, O 14.91.

5-(9H-carbazol-9-yl)-2-(diphenylphosphoryl)benzoic acid (CzPPOA): The synthetic procedure was analogous to that of TPPOA, with the substitution of CzPPOM (2.286 g, 5 mmol) for TPPOM. The reaction produced 0.9 g of white powder with a 40% yield. ^{1}H NMR (TMS, DMSO-d_6, 400 MHz): δ = 13.386 (s, 1H), 8.256 (d, J = 7.6 Hz, 2H), 8.090 (t, J = 2.0 Hz, 1H), 7.975 (d, J = 8.4 Hz, 1H), 7.762 (q, J_1 = 12.8 Hz, J_2 = 8.4Hz, 1H), 7.738-7.645 (m, 4H), 7.642-7.588 (m, 2H), 7.588-7.510 (m, 6H), 7.447 (t, J = 7.6 Hz, 2H), 7.314 ppm (t, J = 7.6 Hz, 2H). LDI-TOF: m/z (%): 487.13 (100) [M^+]; elemental analysis (%) for $C_{31}H_{22}NO_3P$: C 76.38, H 4.55, N 2.87, O 9.85; found: C 76.39, H 4.57, N 2.89, O 9.88.

5-(3,6-Di-*tert*-butyl-9H-carbazol-9-yl)-2-(diphenylphosphoryl)benzoic acid (tBCzPPOA): The synthetic procedure was similar to that of TPPOA, except for using tBCzPPOM (2.846 g, 5 mmol) instead of TPPOM. The reaction yielded 1.2 g of white powder with a 40% yield. ^{1}H NMR (TMS, DMSO-d_6, 400 MHz): δ = 13.359 (s, 1H), 8.324 (s, 2H), 8.077 (s, 1H), 7.977 (d, J = 6.8 Hz, 1H), 7.821-7.720 (m, 1H), 7.718-7.631 (m, 4H), 7.629-7.527 (m, 6H), 7.525-7.424 (m, 4H), 1.416 ppm (s, 18H). LDI-TOF: m/z (%): 599.26 (100) [M^+]; elemental analysis (%) for $C_{39}H_{38}NO_3P$: C 78.11, H 6.39, N 2.34, O 8.00; found: C 78.13, H 6.37, N 2.37, O 8.03.

5-(9,9-Dimethylacridin-10(9H)-yl)-2-(diphenylphosphoryl)benzoic acid (DMACPPOA): The synthetic procedure was similar to that of TPPOA, except that DMACPPOM (2.496 g, 5 mmol) was used instead of TPPOM. The reaction gave 1.0 g of pale yellow powder with a 40% yield. ^{1}H NMR (TMS, $CDCl_3$, 400 MHz): δ =

8.392 (s, 1H), 7.750-7.548 (m, 9H), 7.545-7.432 (m, 5H), 7.324-7.254 (m, 2H), 7.252-7.175 (m, 2H), 7.128 (t, *J* = 7.2 Hz, 1H), 7.036 (d, *J* = 7.6 Hz, 1H), 1.486 ppm (s, 6H). LDI-TOF: m/z (%): 529.18 (100) [M^+]; elemental analysis (%) for $C_{34}H_{28}NO_3P$: C 77.11, H 5.33, N 2.64, O 9.06; found: C 77.11, H 5.32, N 2.67, O 9.08.

5-(9,9-Diphenylacridin-10(9H)-yl)-2-(diphenylphosphoryl)benzoic acid (DPACPPOA): The synthetic procedure was similar to that of TPPOA, except that DMACPPOM (3.116 g, 5 mmol) was used instead of TPPOM. The reaction yielded 1.3 g of white powder with a 40% yield. ^{1}H NMR (TMS, $CDCl_3$, 400 MHz): δ = 8.097 (s, 1H), 7.652-7.527 (m, 6H), 7.524-7.423 (m, 4H), 7.294-7.165 (m, 6H), 7.106 (t, *J* = 7.2 Hz, 2H), 7.028 (q, J_1 = 14.0 Hz, J_2 = 8.0 Hz, 1H), 7.000-6.854 (m, 9H), 6.572 ppm (d, *J* = 8.0 Hz, 2H). LDI-TOF: m/z (%): 653.21 (100) [M^+]; elemental analysis (%) for $C_{44}H_{32}NO_3P$: C 80.84, H 4.93, N 2.14, O 7.34; found: C 80.86, H 4.92, N 2.16, O 7.38.

$NaGd_{(1-x)}F_4$:Tb/Eu_x@OA nanoparticles: Lanthanide nanoparticles were synthesized according to a well-documented co-precipitation method.[1] In a typical experiment for synthesizing $NaGd_{(1-x)}F_4$:Tb_x nanoparticles, $GdCl_3 \cdot 6H_2O$ (1-x mmol) and $TbCl_3 \cdot 6H_2O$ or $EuCl_3 \cdot 6H_2O$ (x mmol) were mixed with oleic acid (OA, 6 mL) and 1-octadecene (15 mL) in a 100-mL flask. The mixture was heated to 140 °C for 3 h. After cooling to 50 °C, a methanol solution (10 mL) containing NaOH (0.1 g, 2.5 mmol) and NH_4F (0.148 g, 4 mmol) was added, and the mixed solution was stirred for 12 h. The temperature was then raised to 70 °C to remove methanol. After that, the solution was heated to 240 °C under an argon atmosphere for 45 min, followed by cooling to room temperature. The resulting nanoparticles were extracted by repeated precipitation with a mixture of ethanol and hexane, collected by centrifugation at 12,000 rpm for 5 min, and re-dispersed in 9 mL of hexane.

$NaGd_{0.6}F_4$:$Tb_{0.4-x}Eu_x$@OA nanoparticles: The synthesis followed the same procedure as above, with the inclusion of $EuCl_3 \cdot 6H_2O$ (x mmol, x = 0.01, 0.05, 0.08, or 0.10).

Preparation of ligand-free nanoparticles: In a typical process,[2] 1 mL of the as-prepared OA-capped nanoparticles dispersion in hexane (~50 mg/mL) was combined with 1 mL of a DMF solution containing $NOBF_4$ (0.011g, 0.1 mmol) at room temperature. The mixture was ultrasonicated for 20 min to remove oleate ligands on the surface, followed by the addition of 1 mL of toluene and further sonication for another 20 min. The ligand-free nanoparticles were collected by centrifugation and redispersed in DMF (1 mL). For purification, 1 mL of a hexane-toluene solution (1:1 v/v) was added to flocculate the dispersion, and the precipitate was collected via centrifugation. The nanoparticles were then redispersed in 2 mL of EtOH to form a stable colloidal dispersion.

Surface ligand modification: For ligand modification, sodium hydroxide (0.002 g, 0.05 mmol) in 1 mL of ethanol was added to the desired ligand (0.05 mmol) in 2 mL of ethanol to prepare a ligand salt solution. This

solution was added to an ethanol dispersion of ligand-free nanoparticles (0.001 mmol) and ultrasonicated for two hours to ensure ligand coordination to nanoparticle surfaces. Excess ligand was removed by centrifugation, and the modified nanoparticles were redispersed in ethanol for optical measurements or in DMF for device fabrication.

Preparation of Tb(ligand)$_3$ complexes: Tb(ligand)$_3$ complexes were prepared according to established protocols.[3] ArPPOA (3 mmol) was dissolved in 10 mL of ethanol, and NaOH (0.120 g, 3 mmol) in aqueous solution (1 M) was added to deprotonate ArPPOA. $TbCl_3{\cdot}6H_2O$ (0.373 g, 1 mmol) in 0.1 mL of water was added dropwise, then the solution was stirred at 60 °C for two hours. The product was purified by precipitation using a concentrated ethanol-water solution.

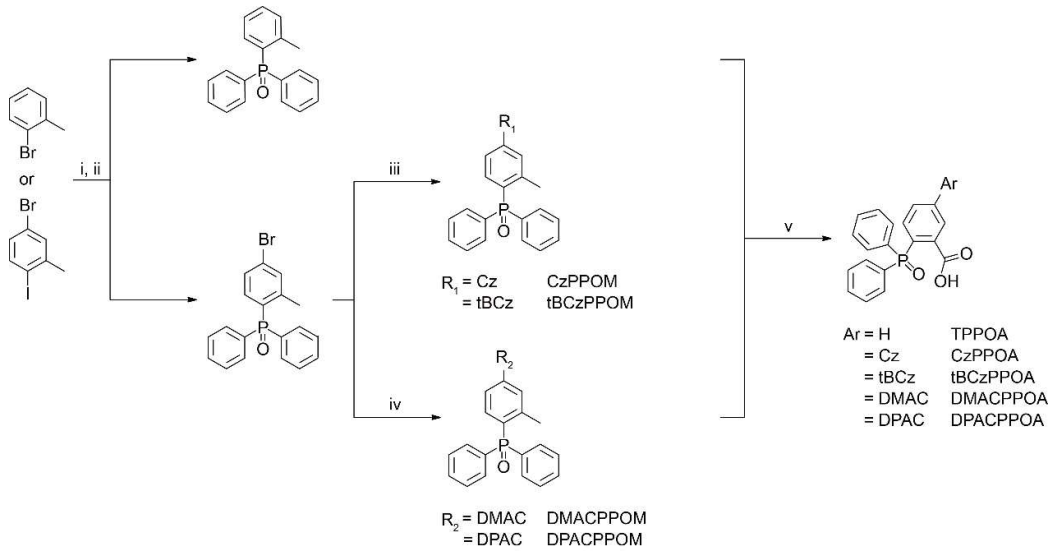

Supplementary Fig. 1. Synthetic procedures of TPPOA, CzPPOA, tBCzPPOA, DMACPPOA and DPACPPOA. i. Mg, Et_2O, 40 °C, 1 h; Ph_2PCl, Et_2O, 0 °C, 12 h; ii. 30% H_2O_2, CH_2Cl_2, 0 °C, 4 h; iii. carbazole/3,6-di-tert-butyl-carbazole, K_2CO_3, CuI, DMI, 190 °C, 12h; iv. $Pd_2(dba)_3$, (*t*-Bu)$_3$P, toluene, room temperature, 20 min; 9,9-dimethyl-9,10-dihydroacridine/9,9-diphenyl-9,10-dihydroacridine, *t*-BuONa, 90 °C, 6 h; v. $KMnO_4$, pyridine, H_2O, 6 h.

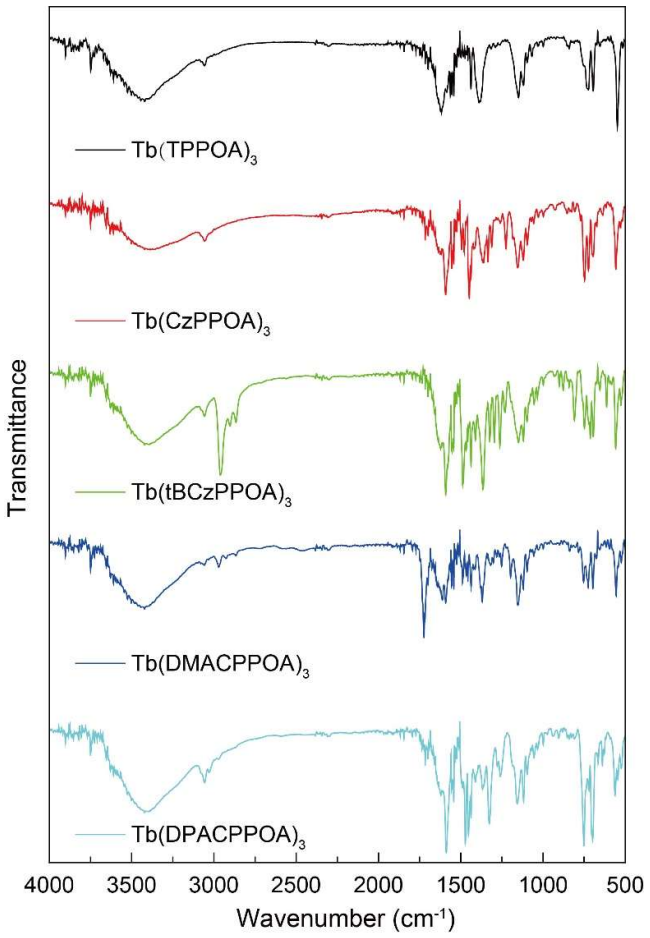

Supplementary Fig. 2. Fourier-transform infrared spectra of $Tb(TPPOA)_3$, $Tb(CzPPOA)_3$, $Tb(tBCzPPOA)_3$, $Tb(DMACPPOA)_3$ and $Tb(DPACPPOA)_3$ in KBr pellets. The peaks around 1150 cm^{-1} and 1437 cm^{-1} are assigned to the characteristic absorption peaks originating from P=O and C-P in ArPPOA. In addition the peaks around 1472 and 1576 cm^{-1} are attributed to the symmetric (ν_s) and asymmetric (ν_{as}) modes of the carboxyl groups (-COO-). The band around 1716 cm^{-1} arises from the stretching vibration of the C=O group.

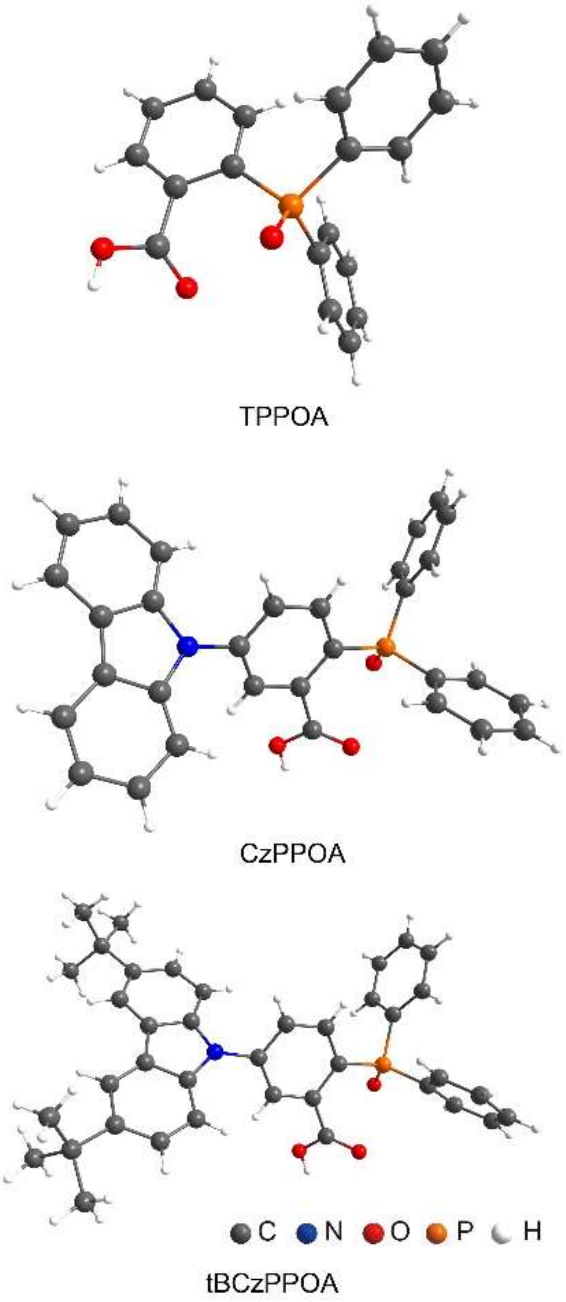

Supplementary Fig. 3. Single-crystal structures of TPPOA, CzPPOA and tBCzPPOA.

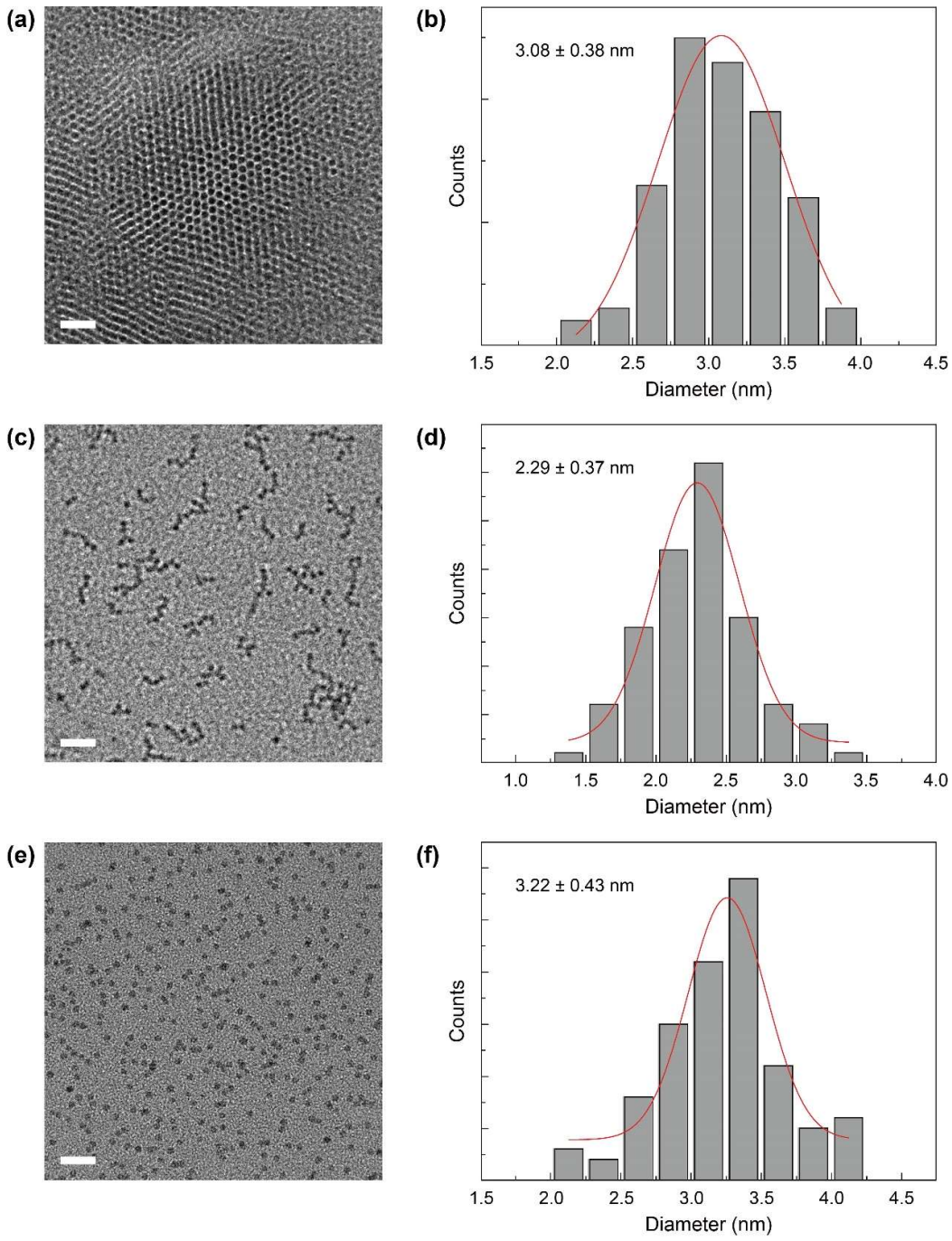

Supplementary Fig. 4. TEM images and corresponding size distribution (right) of $NaGd_{0.6}F_4:Tb_{0.4}$@OA (a, b), $NaGd_{0.6}F_4:Tb_{0.4}$ (c, d), and $NaGd_{0.6}F_4:Tb_{0.4}$@CzPPOA (e, f). The scale bars are 20 nm.

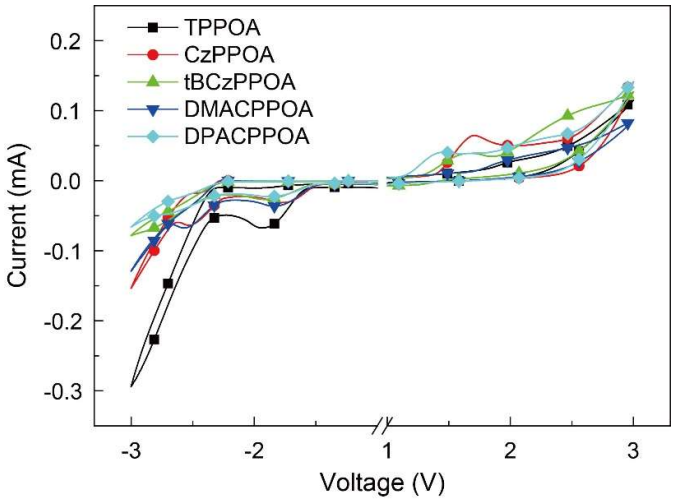

Supplementary Fig. 5. CV curves of TPPOA, CzPPOA, tBCzPPOA, DMACPPOA and DPACPPOA measured at room temperature with a scanning rate of 100 mV/s.

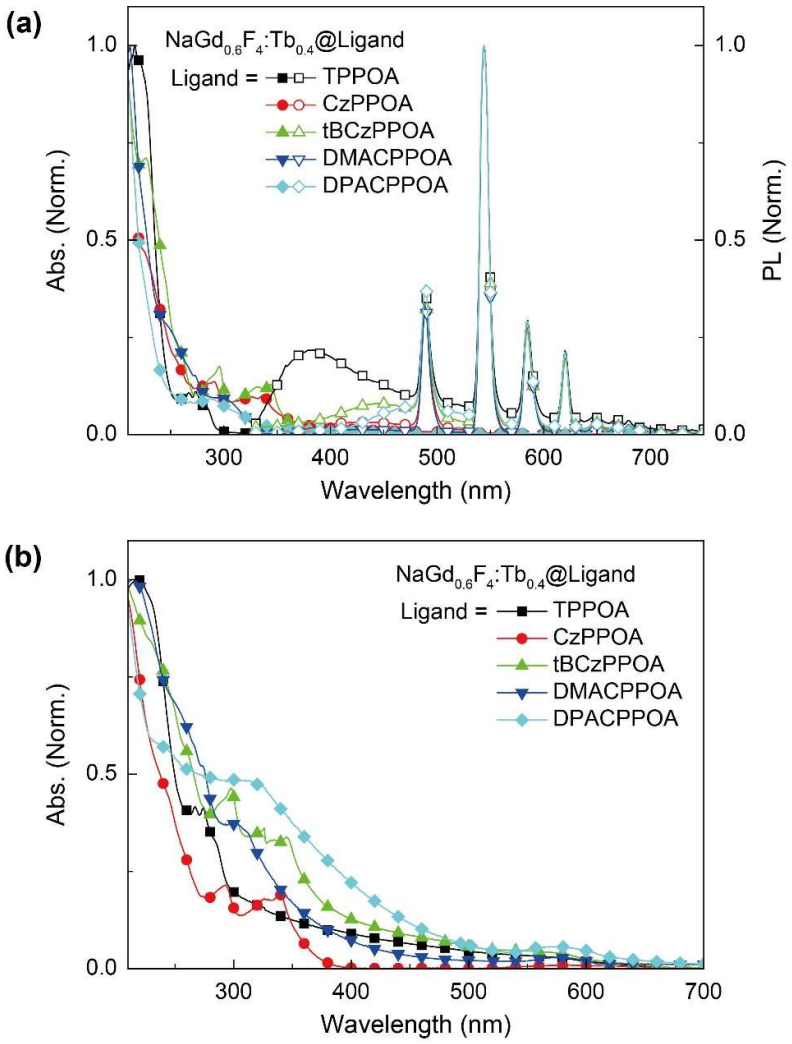

Supplementary Fig. 6. Comparison of the absorption and steady-state PL spectra of $NaGd_{0.6}F_4:Tb_{0.4}$@Ligand in (a) EtOH (2 mg/mL) and (b) films.

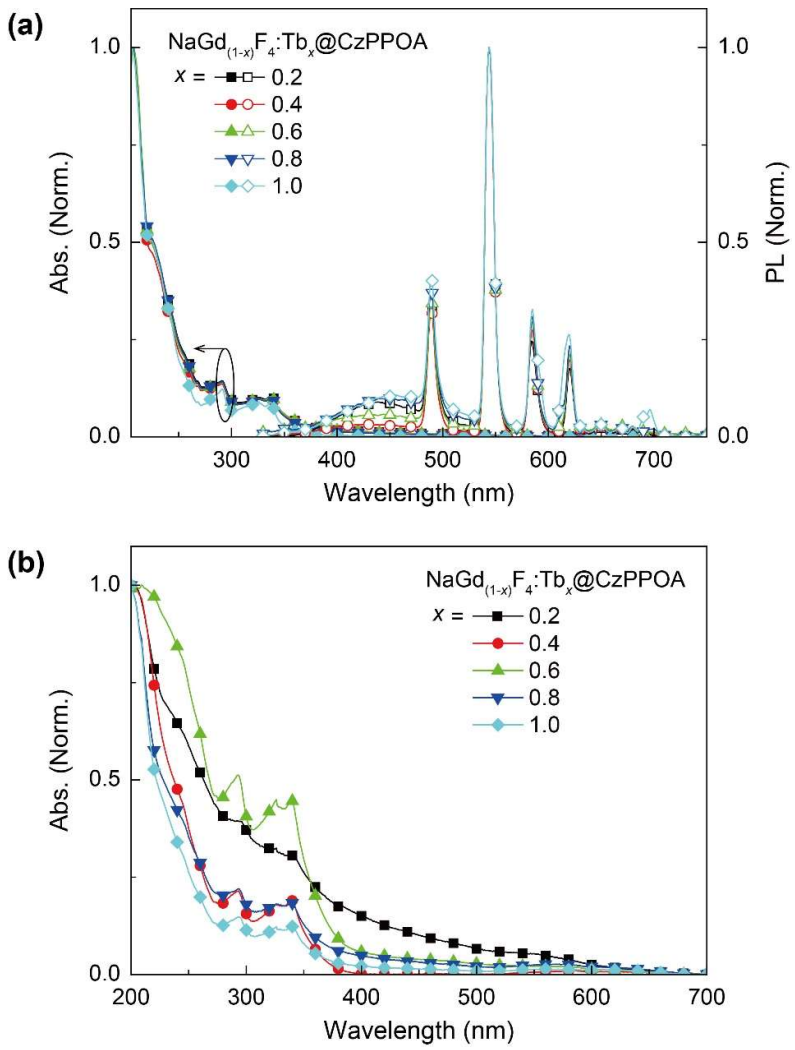

Supplementary Fig. 7. Doping concentration dependence of absorption and steady-state PL spectra for $NaGd_{(1-x)}F_4:Tb_x$@CzPPOA in (a) EtOH (2 mg/mL) and (b) films (x = 0.2-1.0).

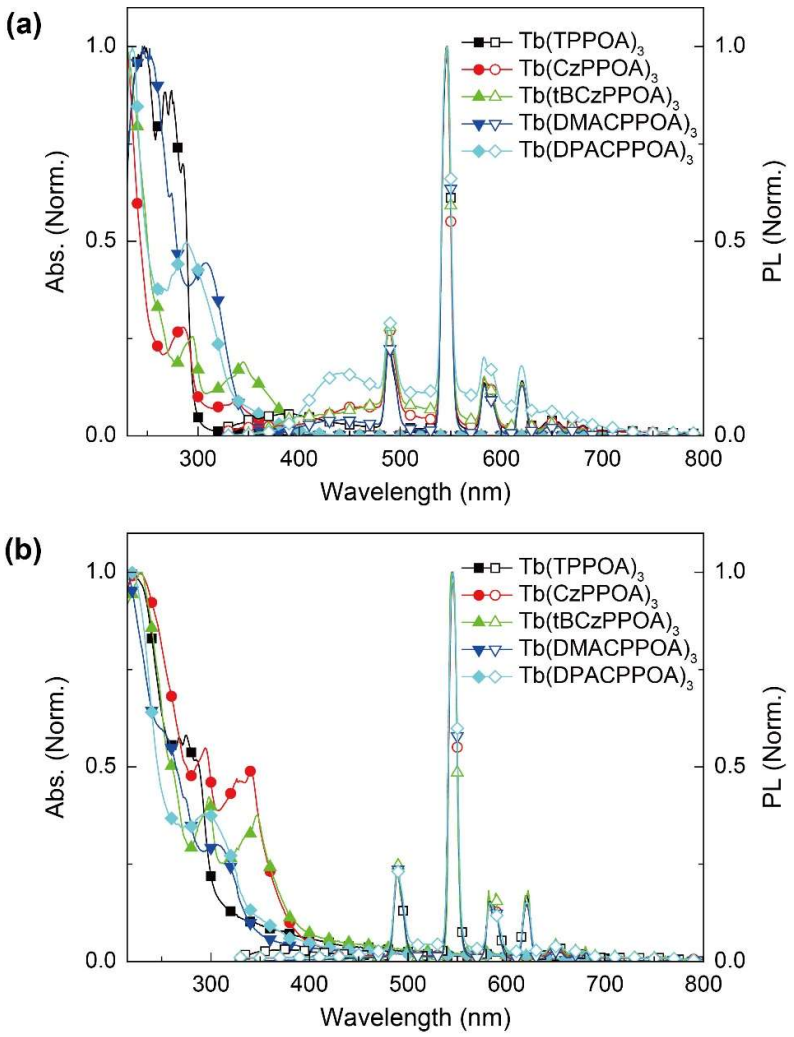

Supplementary Fig. 8. Absorption and steady-state PL spectra for $Tb(Ligand)_3$ in (a) CH_2Cl_2 (10^{-5} g/mL) and (b) $Tb(Ligand)_3$ films.

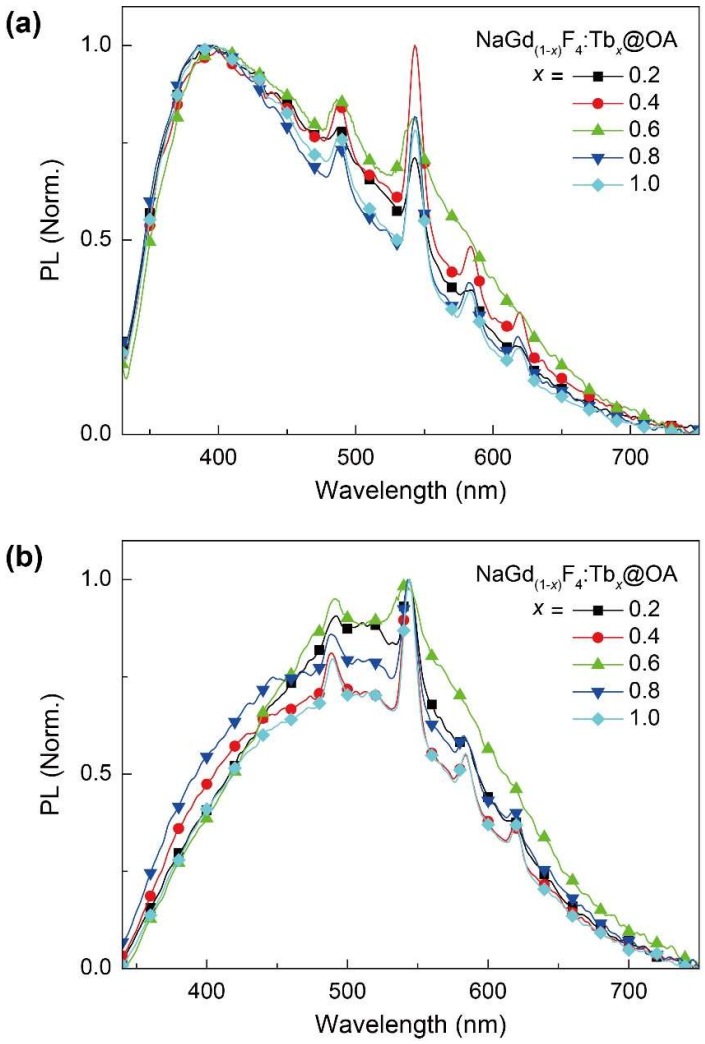

Supplementary Fig. 9. Steady-state PL spectra of $NaGd_{(1-x)}F_4:Tb_x$@OA (x = 0.2-1.0) in (a) hexane (10^{-3} g/mL) and (b) neat films.

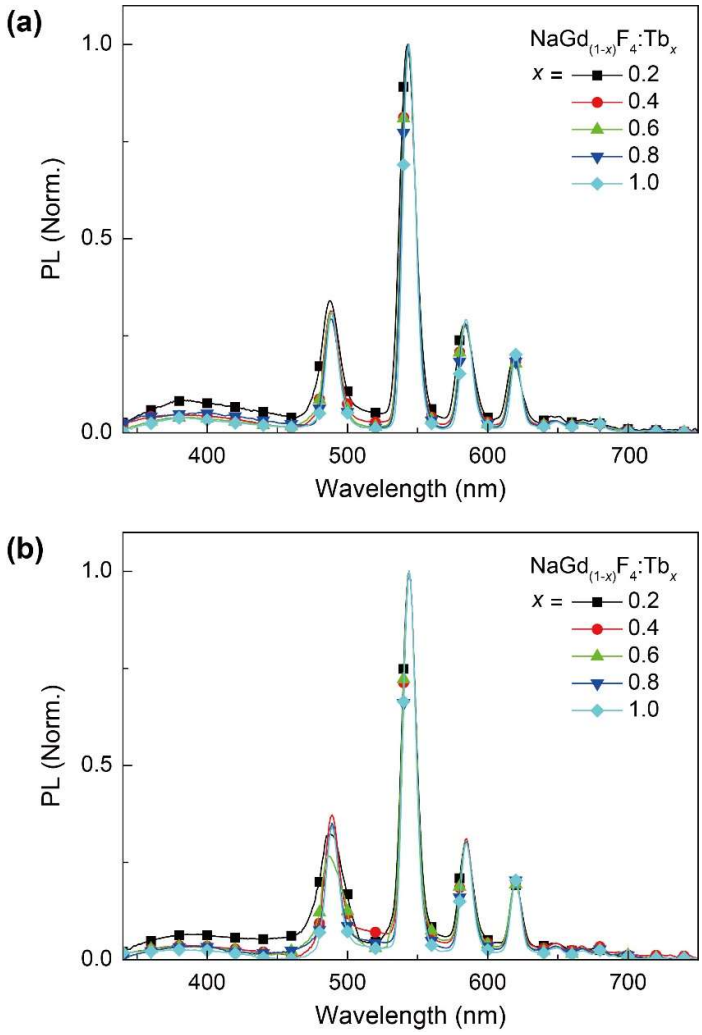

Supplementary Fig. 10. Steady-state PL spectra of $NaGd_{(1-x)}F_4:Tb_x$ (x = 0.2-1.0) in (a) EtOH (10^{-2} g/mL) and (b) neat films.

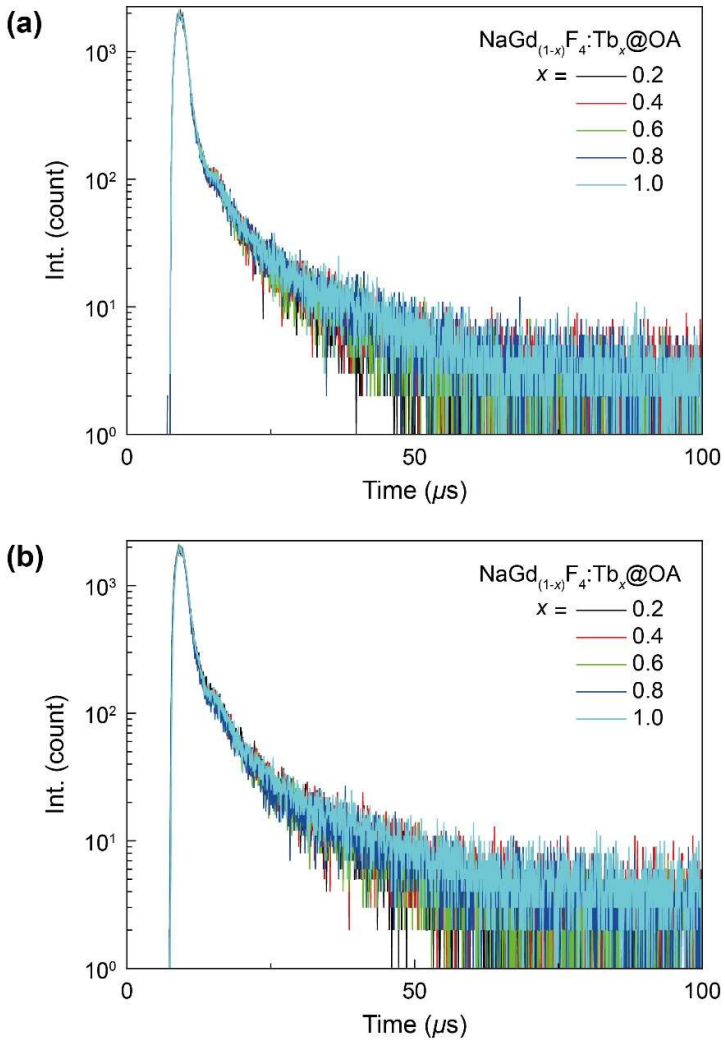

Supplementary Fig. 11. Decay curves of $NaGd_{(1-x)}F_4:Tb_x$@OA (x = 0.2-1.0) in (a) hexane (10^{-3} g/mL) and (b) neat films at 544 nm.

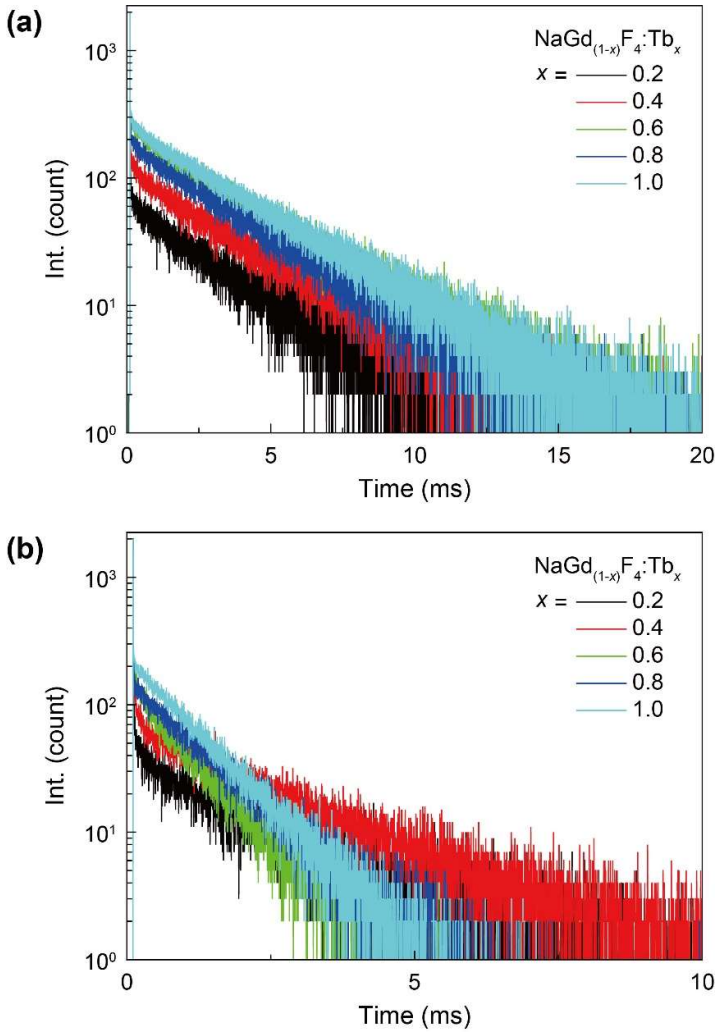

Supplementary Fig. 12. Decay curves of $NaGd_{(1-x)}F_4:Tb_x$ (x = 0.2-1.0) in (a) EtOH (10^{-2} g/mL) and (b) neat films at 544 nm.

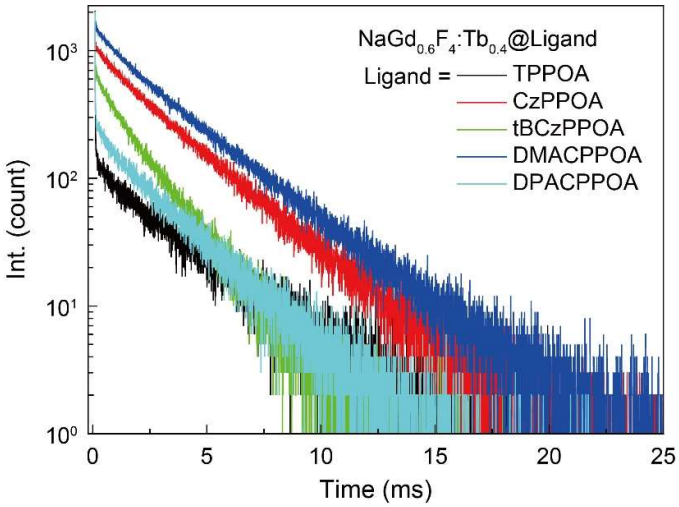

Supplementary Fig. 13. Time decay curves of $NaGd_{0.6}F_4:Tb_{0.4}$@Ligand in EtOH (2 mg/mL) at 544 nm.

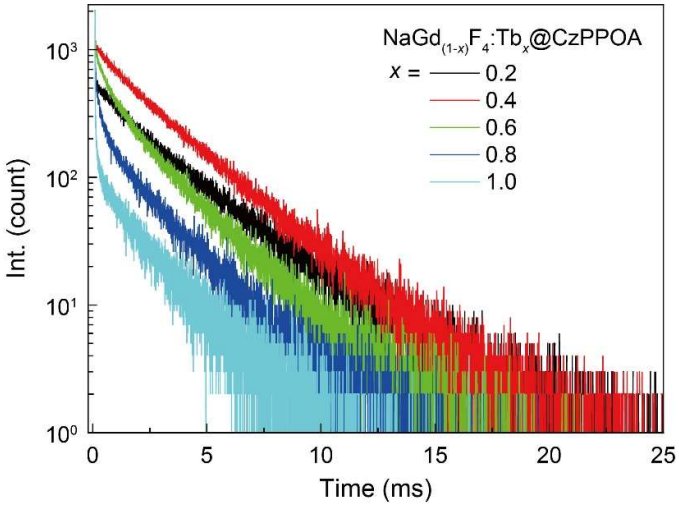

Supplementary Fig. 14. Doping concentration dependence of time decay curves for $NaGd_{(1-x)}F_4:Tb_x$@CzPPOA in EtOH (2 mg/mL) (x = 0.2-1.0) at 544 nm.

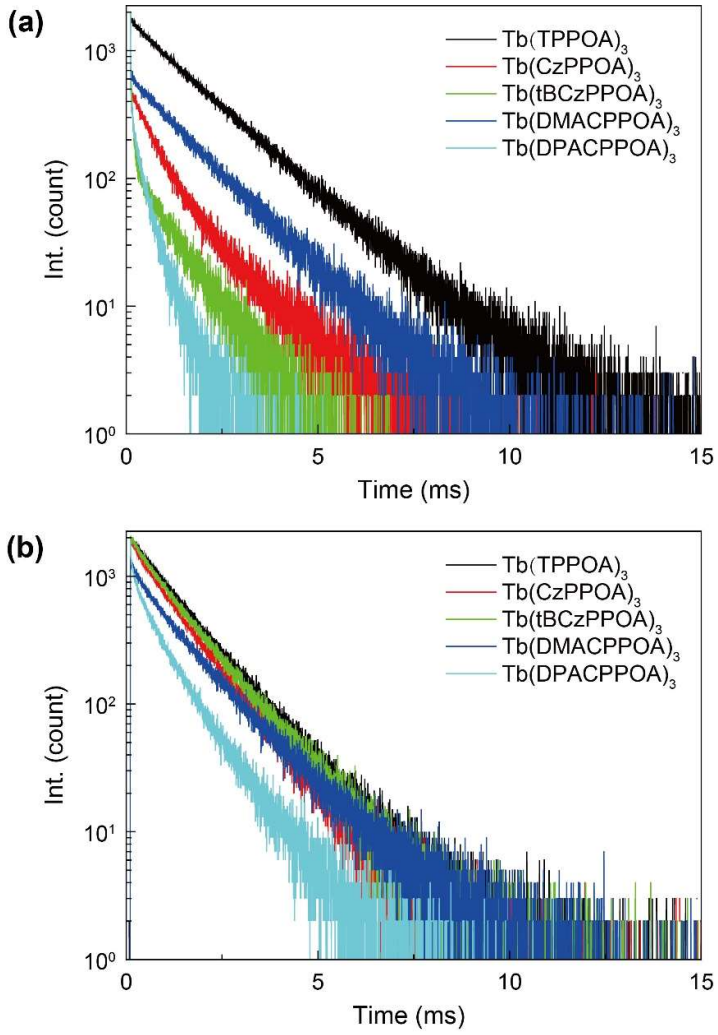

Supplementary Fig. 15. Time decay curves for $Tb(Ligand)_3$ in (a) CH_2Cl_2 (10^{-5} g/mL) and (b) films at 544 nm.

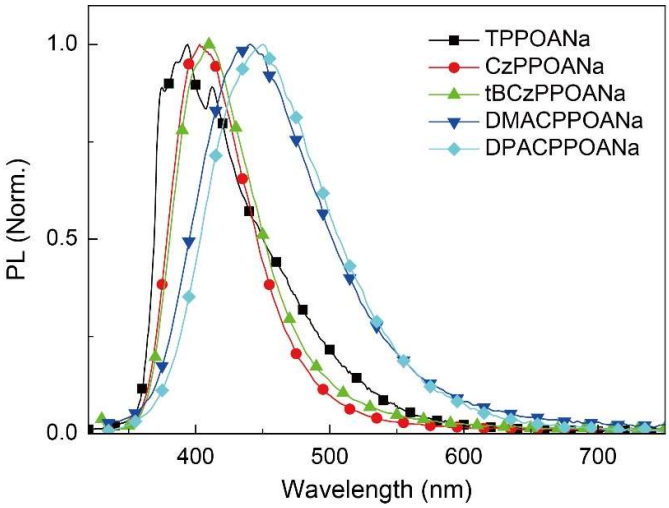

Supplementary Fig. 16. Steady-state PL spectra of sodium carboxylates for the ligands TPPOANa, CzPPOANa, tBCzPPOANa, DMACPPOANa and DPACPPOANa.

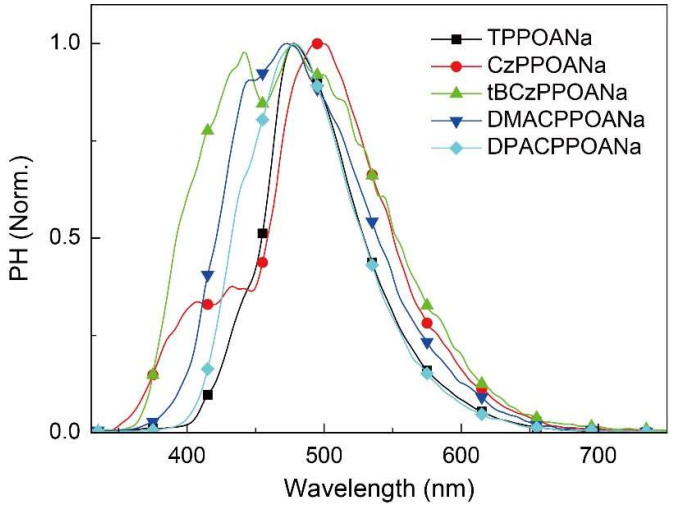

Supplementary Fig. 17. Phosphorescence (PH) spectra of sodium carboxylates for the ligands TPPOANa, CzPPOANa, tBCzPPOANa, DMACPPOANa and DPACPPOANa in film form at 50 K. The PH spectra were measured with time-resolved techniques, with data recorded in the range of 1 ms-10 ms.

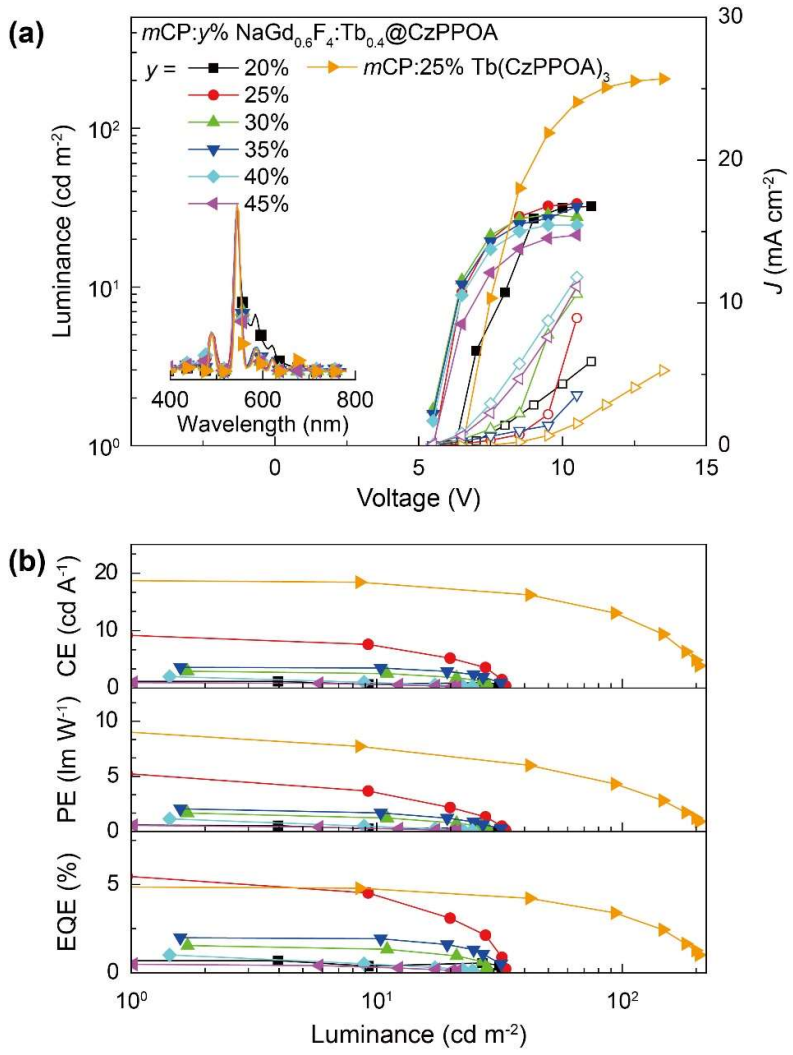

Supplementary Fig. 18. (a) EL spectra (inset) and Current density-voltage-luminance (J-V-L) characteristics of *m*CP:*y*% $NaGd_{0.6}F_4$:$Tb_{0.4}$@CzPPOA at different values of *y*, as well as *m*CP:25% $Tb(CzPPOA)_3$. (b) Efficiency *vs.* Luminance relationships.

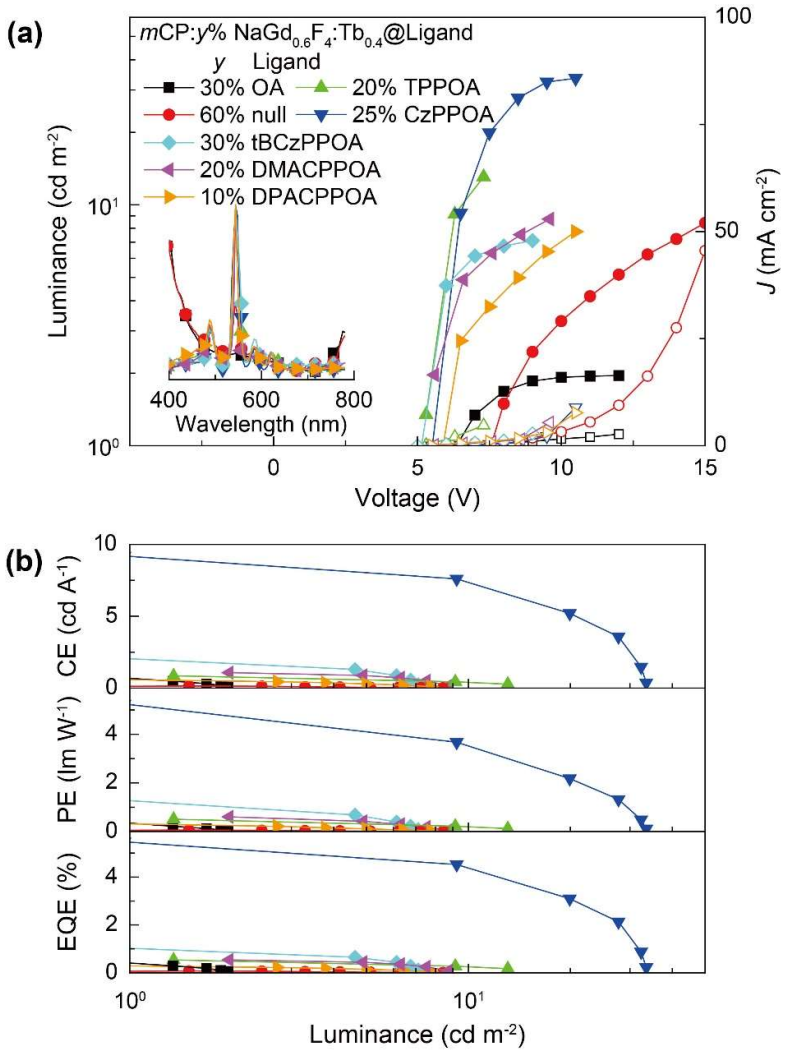

Supplementary Fig. 19. (a) EL spectra (inset) and current density-voltage-luminance (J-V-L) characteristics of *m*CP:*y*% $NaGd_{0.6}F_4:Tb_{0.4}$@Ligand at different values of *y*. (b) Efficiency *vs.* Luminance relationships.

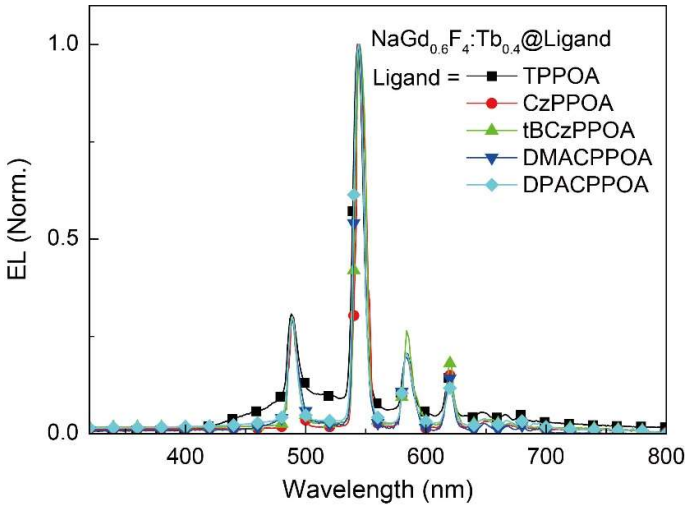

Supplementary Fig. 20. Electroluminescence spectra of $NaGd_{0.6}F_4:Tb_{0.4}$@Ligand.

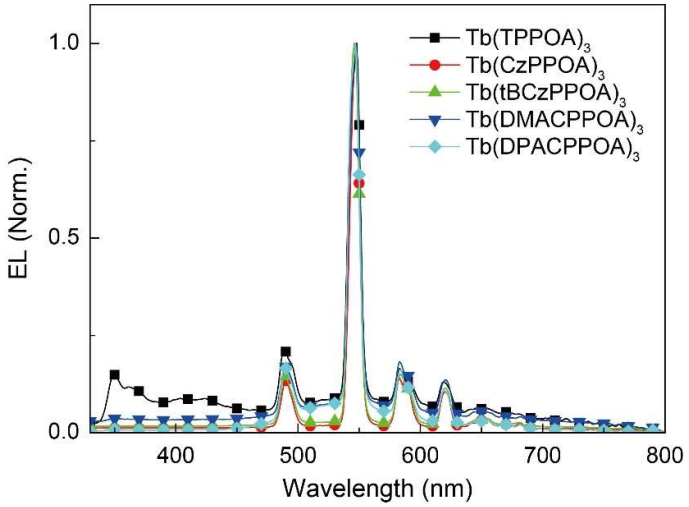

Supplementary Fig. 21. Electroluminescence spectra of $Tb(Ligand)_3$.

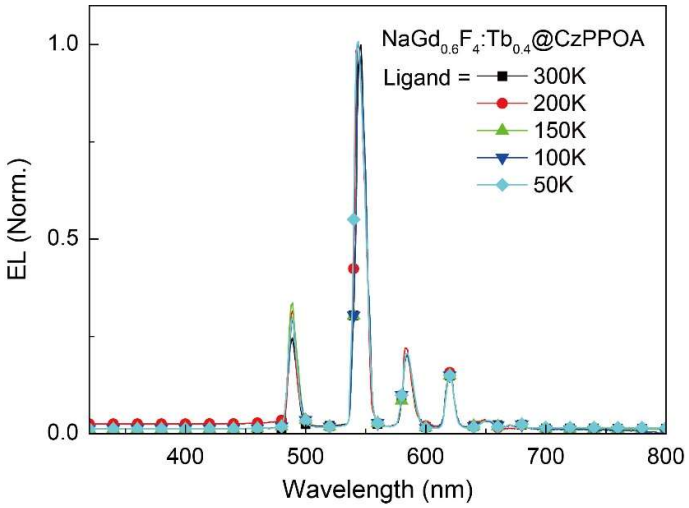

Supplementary Fig. 22. Temperature dependence of electroluminescence spectra for $NaGd_{0.6}F_4:Tb_{0.4}$@CzPPOA in the range of 50-300 K.

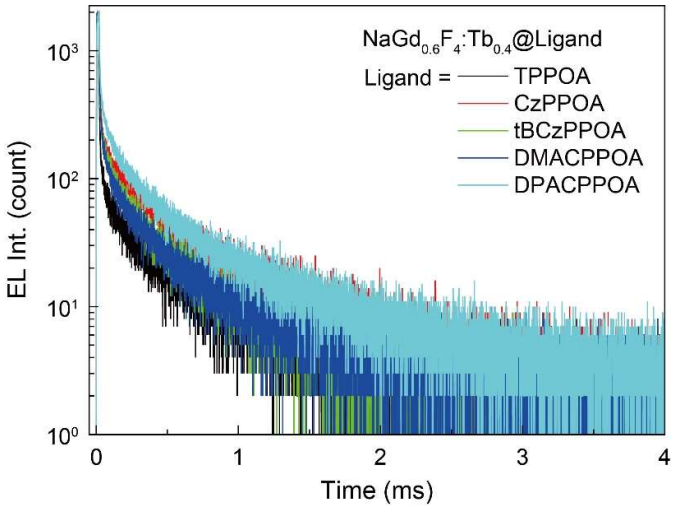

Supplementary Fig. 23. Electroluminescent time decays of $NaGd_{0.6}F_4:Tb_{0.4}$@Ligand.

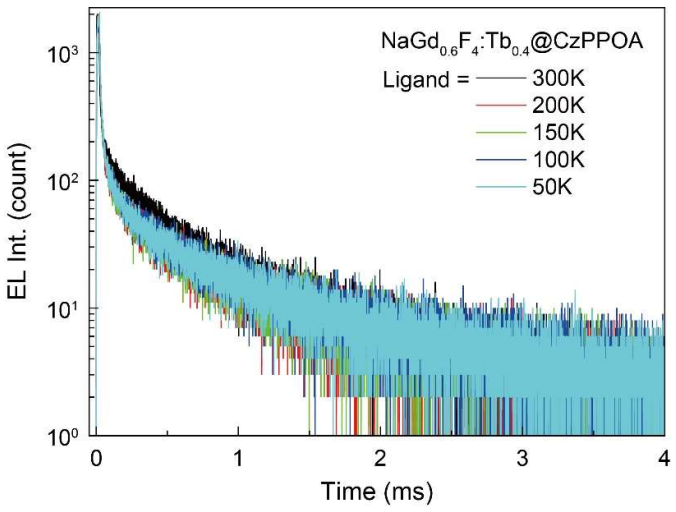

Supplementary Fig. 24. Electroluminescent time decays of $NaGd_{0.6}F_4:Tb_{0.4}$@CzPPOA in the range of 50-300 K.

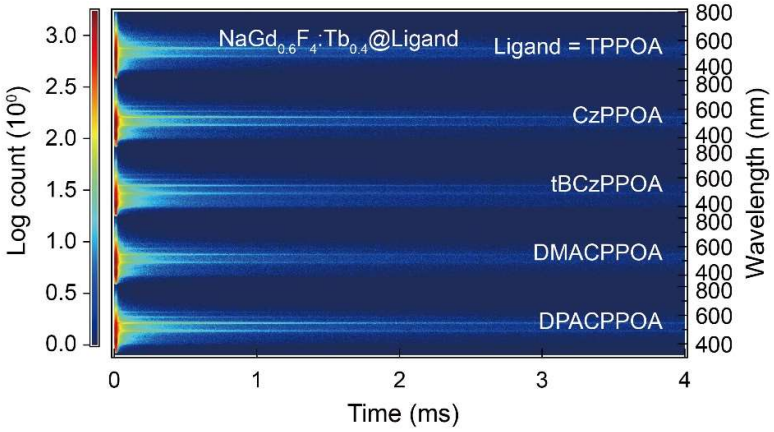

Supplementary Fig. 25. Time-resolved EL emission spectra of $NaGd_{0.6}F_4:Tb_{0.4}$@Ligand.

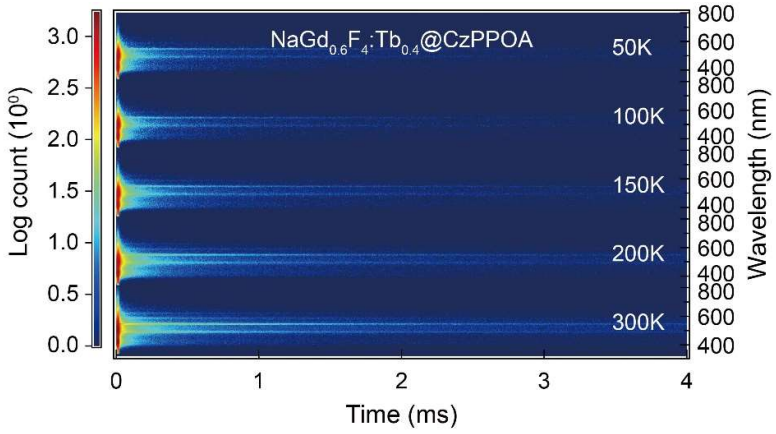

Supplementary Fig. 26. Time-resolved EL emission spectra of $NaGd_{0.6}F_4:Tb_{0.4}$@CzPPOA in the range of 50-300 K.

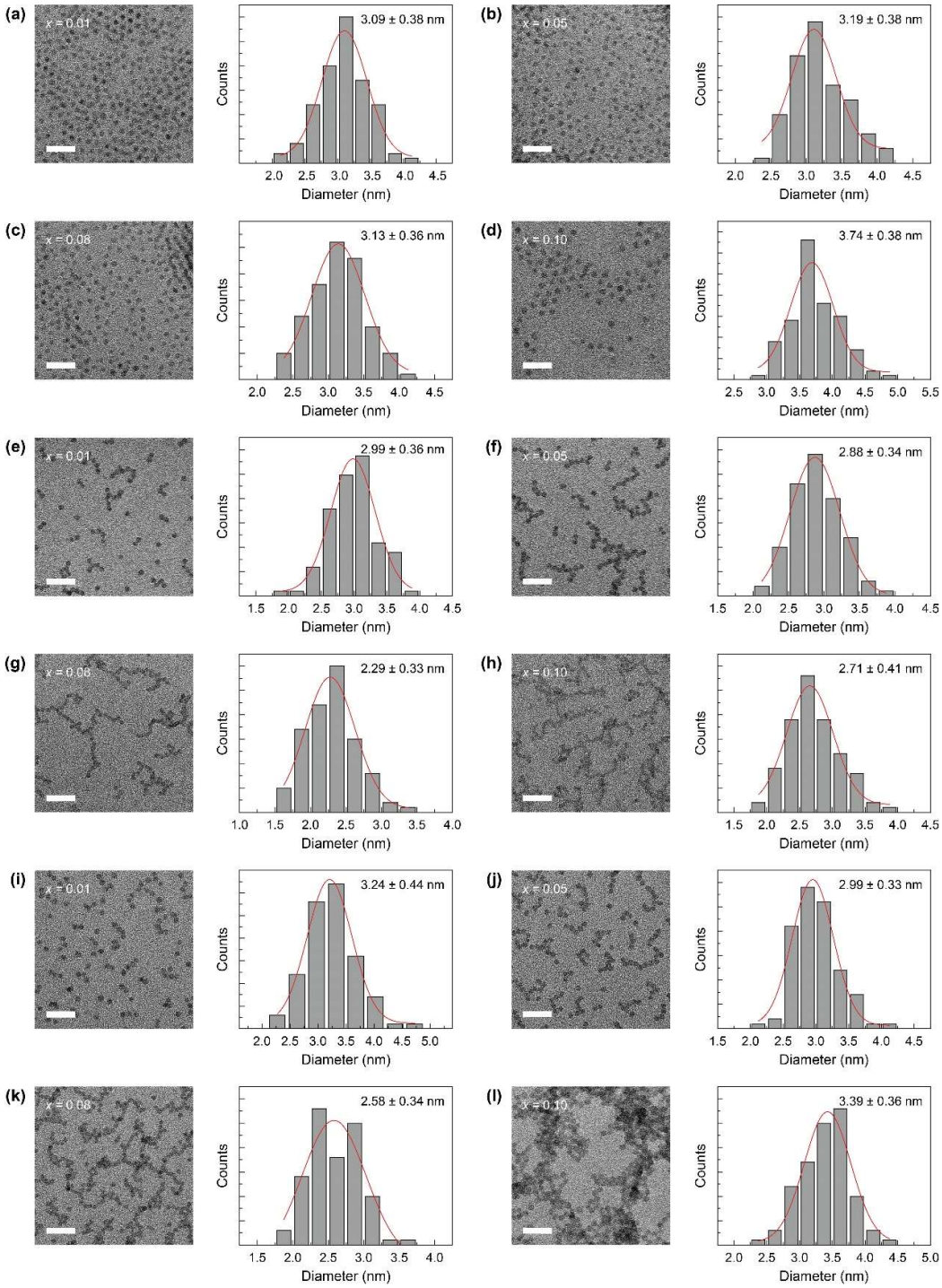

Supplementary Fig. 27. TEM images and corresponding size distribution of $NaGd_{0.6}F_4:Tb_{0.4-x},Eu_x$@OA (a, b, c, d), $NaGd_{0.6}F_4:Tb_{0.4-x},Eu_x$ (e, f, g, h), and $NaGd_{0.6}F_4:Tb_{0.4-x},Eu_x$@CzPPOA (i, j, k, l) ($x$ = 0.01, 0.05, 0.08, 0.10). The scale bars are 20 nm.

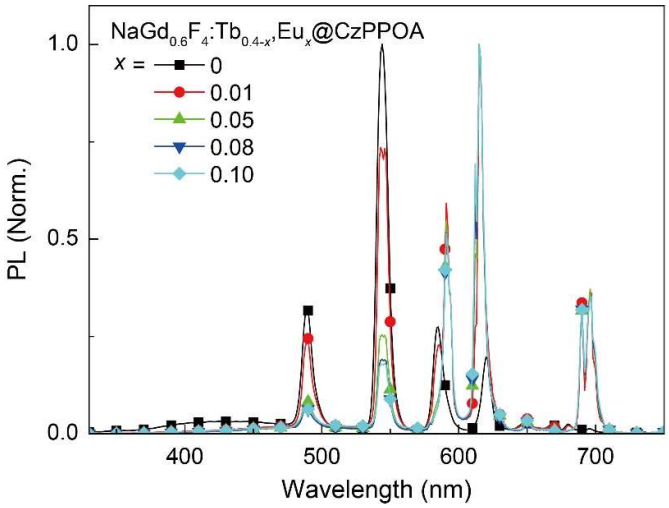

Supplementary Fig. 28. Steady-state photoluminescence (PL) spectra for $NaGd_{0.6}F_4:Tb_{0.4-x},Eu_x$@CzPPOA in EtOH (2 mg/mL) (x = 0-1.0).

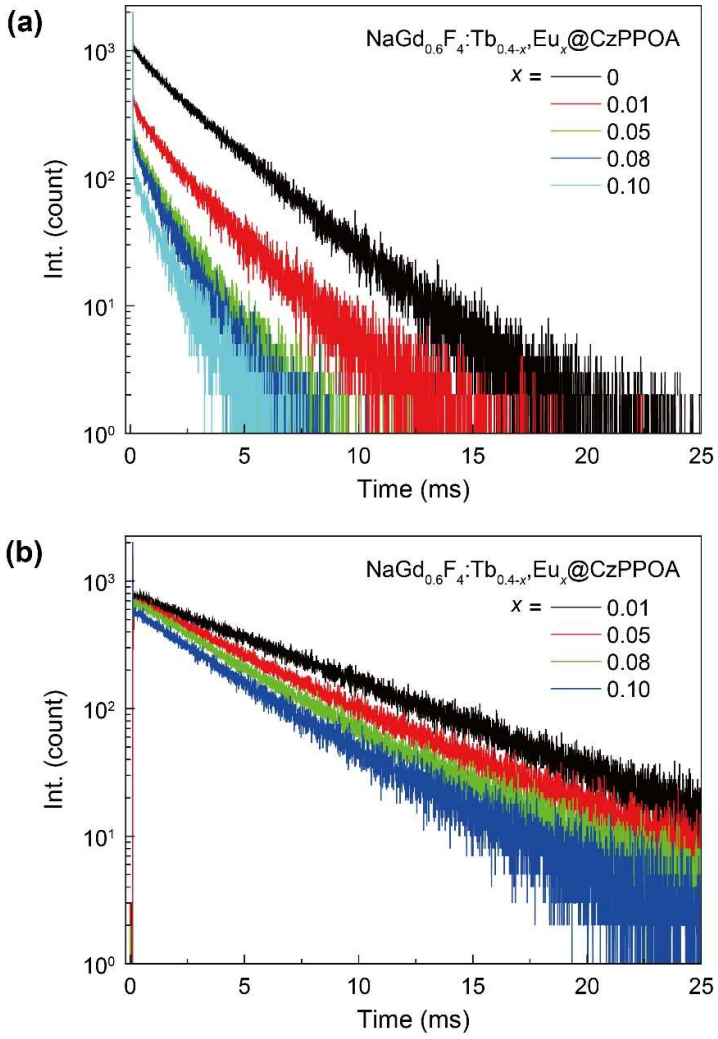

Supplementary Fig. 29. Doping concentration dependence of time decay curves for $NaGd_{0.6}F_4:Tb_{0.4-x},Eu_x$@CzPPOA in EtOH (2 mg/mL) at 544 nm (a) and 615 nm (b) (x = 0-0.10).

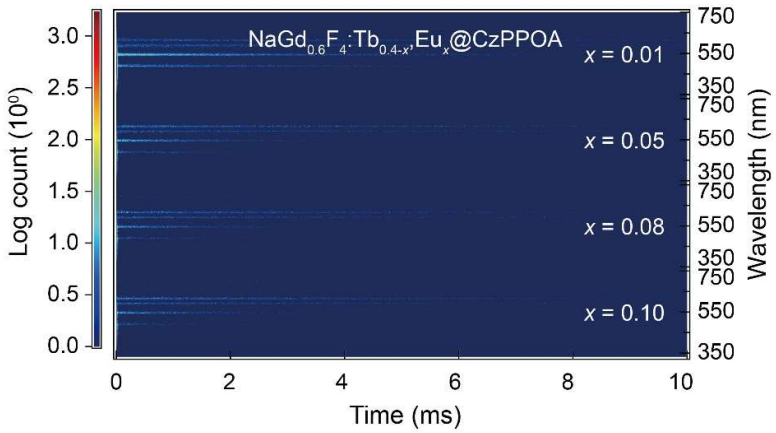

Supplementary Fig. 30. Doping concentration dependence of time-resolved emission spectra (TRES) for $NaGd_{0.6}F_4:Tb_{0.4-x},Eu_x$@CzPPOA in EtOH (2 mg/mL) (x = 0.01-0.10).

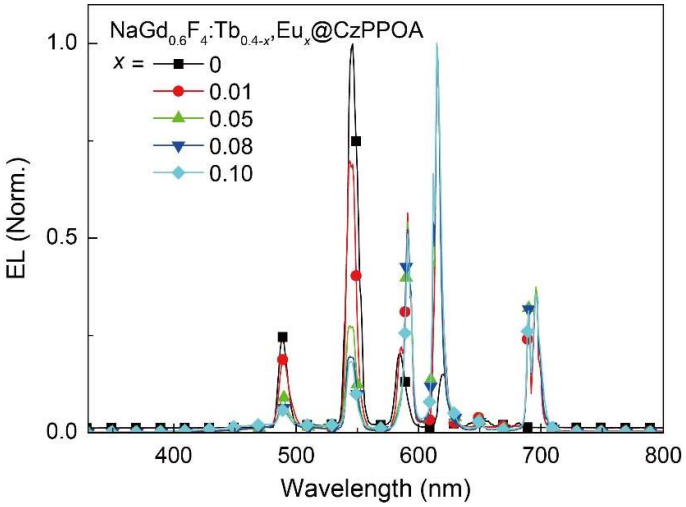

Supplementary Fig. 31. Doping concentration dependence of electroluminescence spectra for $NaGd_{0.6}F_4:Tb_{0.4-x}Eu_x$@CzPPOA ($x$ = 0-0.10).

Supplementary Table S1. Photophysical parameters of $NaGd_{1-x}F_4:Tb_x$@Ligand.

Ligand	x	$\lambda_{Abs.}$[a] (nm)	λ_{PL}[d] (nm)	η_{PL}[g] (%)	τ[h] (ms)
OA	0.2	-	487, 543, 584, 616[e] 492, 544, 584, 618[c]	-	0.0009, 0.0109[e] 0.0010, 0.0114[c]
	0.4	-	488, 543, 584, 619[e] 489, 544, 584, 619[c]	-	0.0009, 0.0117[e] 0.0010, 0.0121[c]
	0.6	-	489, 542, 584, 620[e] 491, 543, 584, 619[c]	-	0.0008, 0.0135[e] 0.0009, 0.0114[c]
	0.8	-	488, 543, 584, 618[e] 488, 544, 583, 617[c]	-	0.0011, 0.0102[e] 0.0009, 0.0115[c]
	1.0	-	488, 543, 583, 619[e] 489, 544, 584, 620[c]	-	0.0009, 0.0119[e] 0.0009, 0.0114[c]
Null	0.2	-	487, 543, 583, 619[f] 488, 544, 584, 619[c]	-	0.0020, 2.5301[f] 0.0022, 1.9242[c]
	0.4	-	488, 543, 584, 619[f] 489, 544, 585, 620[c]	-	0.0033, 3.0244[f] 0.0035, 2.0935[c]
	0.6	-	488, 543, 584, 619[f] 486, 544, 584, 620[c]	-	0.0038, 3.1369[f] 0.0017, 0.8223[c]
	0.8	-	488, 543, 584, 620[f] 489, 544, 585, 620[c]	-	0.0015, 2.9755[f] 0.0017, 1.0421[c]
	1.0	-	489, 544, 584, 620[f] 489, 544, 585, 620[c]	-	0.0015, 3.1585[f] 0.0016, 0.9159[c]
TPPOA	0.4	216, 229, 262, 267, 274, 284[b] 218, 231, 260, 267, 274, 287[c]	489, 544, 585, 620[b] 488, 543, 584, 620[c]	- 0.76	0.0036, 2.8314[b] 0.0029, 2.3458[c]
CzPPOA	0.2	226, 244, 259, 268, 273, 285, 291, 326, 330, 333, 338[b] 223, 244, 261, 268, 273, 286, 293, 326, 329, 332, 339[c]	489, 544, 584, 620[b] 489, 544, 584, 620[c]	- 22.59	0.0035, 3.0224[b] 0.0048, 2.4564[c]
	0.4	225, 244, 260, 268, 274, 285, 291, 326, 337[b]	489, 544, 585, 620[b]	-	0.0036, 2.7582[b]

	0.6	225, 244, 260, 267, 274, 285, 293, 326, 332, 339[c]	489, 544, 585, 620[c]	25.51	--, 2.5520[c]
		225, 244, 261, 268, 274, 285, 291, 326, 337[b]	489, 544, 585, 620[b]	-	0.0046, 2.0304[b]
	0.8	221, 244, 260, 267, 274, 286, 293, 326, 329, 339[c]	489, 544, 585, 620[c]	15.07	--, 1.0179[c]
		225, 244, 261, 268, 274, 284, 291, 326, 338[b]	489, 544, 585, 620[b]	-	0.0048, 2.0193[b]
		222, 245, 260, 269, 274, 286, 293, 326, 328, 332, 338[c]	489, 544, 585, 620[c]	8.93	--, 0.4517[c]
	1.0	225, 244, 261, 268, 274, 284, 291, 325, 337[b]	489, 544, 585, 619[b]	-	0.0037, 1.9101[b]
		226, 245, 260, 268, 273, 286, 293, 326, 332, 339[c]	489, 544, 585, 616[c]	7.97	--, 0.3289[c]
tBCzPPOA	0.4	227, 245, 260, 273, 285, 296, 326, 332, 343[b]	489, 544, 585, 620[b]	-	0.0035, 1.7653[b]
		229, 246, 261, 275, 286, 298, 313, 326, 332, 334, 345[c]	489, 544, 585, 620[c]	5.49	0.0039, 2.4863[c]
DMACPPOA	0.4	212, 229, 253, 266, 273, 292, 298, 301, 308 [b]	489, 544, 584, 620[b]	-	0.0019, 2.9946[b]
		214, 230, 255, 266, 273, 293, 298, 303, 308, 312, 326[c]	489, 544, 584, 620[c]	4.09	0.0041, 2.0405[c]
DPACPPOA	0.4	219, 232, 255, 261, 267, 274, 286, 289, 293, 296, 303, 311, 317, 324[b]	489, 544, 585, 620[b]	-	0.0035, 2.4748[b]
		222, 235, 256, 260, 266, 274, 286, 289, 292, 299, 303, 310, 317, 324[c]	489, 544, 585, 620[c]	6.56	0.0040, 1.8523[c]

[a] Absorption peak wavelength; [b] in EtOH solution (2 mg/mL); [c] in film form; [d] Photoluminescence peak wavelength; [e] in *n*-hexane solution (10^{-3} g/mL); [f] in EtOH solution (10^{-2} g/mL); [g] absolute PL quantum yield measured with an integrating sphere; [h] lifetimes fitted according to time decays.

Supplementary Table S2. Photophysical parameters of Tb(Ligand)$_3$.

Complex	λ_{Abs}[a] (nm)	λ_{PL}[d] (nm)	η_{PL}[e] (%)	τ[f] (ms)
Tb(TPPOA)$_3$	220, 247, 261, 268, 274, 285[b]	489, 546, 533, 620[b]	--	1.5937[b]
	222, 231, 261, 268, 275, 285[c]	489, 545, 583, 621[c]	0.86	1.1953[c]
Tb(CzPPOA)$_3$	229, 244, 260, 268, 274, 285, 293, 326, 332, 337[b]	489, 546, 533, 621[b]	--	0.9849[b]
	223, 244, 260, 268, 274, 285, 294, 326, 329, 340[c]	490, 546, 583, 620[c]	24.25	1.0613[c]
Tb(tBCzPPOA)$_3$	230, 246, 260, 274, 286, 295, 312, 327, 331, 334, 345[b]	489, 546, 533, 620[b]	--	0.8745[b]
	229, 246, 261, 274, 286, 298, 312, 326, 331, 335, 347[c]	489, 544, 582, 622[c]	21.55	1.1486[c]
Tb(DMACPPOA)$_3$	213, 230, 254, 266, 273, 293, 298, 303, 308, 312, 326[b]	489, 547, 533, 620[b]	--	1.3976[b]
	214, 229, 254, 266, 273, 293, 298, 303, 307, 312, 326[c]	489, 546, 583, 621[c]	15.53	1.2345[c]
Tb(DPACPPOA)$_3$	235, 255, 260, 266, 274, 286, 288, 292, 298, 304, 311, 318, 324[b]	489, 547, 533, 620[b]	--	0.3296[b]
	221, 233, 254, 261, 267, 274, 285, 288, 291, 296, 303, 311, 318, 324[c]	489, 546, 583, 621[c]	12.59	0.8329[c]

[a] Absorption peak wavelength; [b] in CH_2Cl_2 solution (10^{-5} g/mL); [c] in film form; [d] Photoluminescence peak wavelength; [e] absolute PL quantum yield measured with an integrating sphere; [f] lifetimes fitted according to time decays.

Supplementary Table S3. EL performances for devices based on the structures of ITO|PEDOT:PSS (40 nm)|PVK (20 nm)|host:*x* wt% **$NaGd_{0.6}F_4:Tb_{0.4}$@ligand** (25 nm)|DPEPO (10 nm)|TmPyPB (40 nm)|LiF (1 nm)|Al.

Emissive layer	*x*	V_{on}[a]	L_{max}[b] (cd m^{-2})	η_{max}[c]			CIE (x, y)	λ (nm)
				η_{CE} (cd A^{-1})	η_{PE} (lm W^{-1})	η_{EQE} (%)		
*m*CP:*x* wt% $NaGd_{0.6}F_4:Tb_{0.4}$@OA	10	7	4.063	0.4025	0.18055	0.20125	(0.28, 0.3)	400, 544
	20	7	2.112	0.42792	0.19195	0.25675	(0.24, 0.22)	400, 544
	30	6.4	1.956	0.78545	0.41105	0.47127	(0.24, 0.20)	400, 544
	40	6	1.608	0.23925	0.12521	0.1684	(0.22, 0.16)	400, 544
	50	6	1.873	0.3657	0.19138	0.24136	(0.22, 0.15)	400, 544
	60	7.6	1.71	0.44196	0.23129	0.44638	(0.22, 0.17)	400, 544
*m*CP:*x* wt% $NaGd_{0.6}F_4:Tb_{0.4}$	10	7	5.563	0.12354	0.04849	0.06918	(0.23, 0.19)	488, 544, 588, 620
	20	8	1.618	0.06191	0.06895	0.03034	(0.23, 0.21)	488, 544, 584, 620
	30	7.2	3.178	0.09313	0.03364	0.04657	(0.23, 0.19)	488, 544, 584, 620
	40	6.7	3.322	0.15156	0.06694	0.07578	(0.23, 0.20)	488, 544, 584, 620
	50	7.1	6.469	0.12988	0.05211	0.06429	(0.25, 0.26)	488, 544, 584, 620
	60	7.6	8.414	0.14853	0.0583	0.07738	(0.23, 0.26)	488, 544, 584, 620
	70	9.1	6.519	0.05354	0.01681	0.0303	(0.26, 0.29)	488, 544, 584, 620
	80	10.4	4.815	0.01646	0.0048	0.0102	(0.25, 0.32)	488, 544, 584, 620
BCPO:*x* wt% $NaGd_{0.6}F_4:Tb_{0.4}$@CzPPOA	30	6	15.03	0.99506	0.52075	0.498	(0.25, 0.41)	488, 544, 584, 620
	40	6	12.75	0.61184	0.3202	0.309	(0.25, 0.45)	488, 544, 584, 620
	50	6	15.38	0.6293	0.29925	0.318	(0.25, 0.45)	488, 544, 584, 620
	60	6	9.847	0.63056	0.32999	0.323	(0.26, 0.44)	488, 544, 584, 620
CBP:*x* wt% $NaGd_{0.6}F_4:Tb_{0.4}$@CzPPOA	30	6	10.17	0.75358	0.39437	0.54291	(0.29, 0.49)	488, 544, 584, 620
	40	6	13.7	0.62739	0.32833	0.38491	(0.29, 0.47)	488, 544, 584, 620
	50	5.6	13.18	0.87669	0.50051	0.48811	(0.29, 0.47)	488, 544, 584, 620
	60	6	8.379	0.62457	0.35657	0.30935	(0.29, 0.48)	488, 544, 584, 620
CDBP:*x* wt% $NaGd_{0.6}F_4:Tb_{0.4}$@CzPPOA	30	6.2	8.76	1.04917	0.568	0.724	(0.26, 0.43)	488, 544, 584, 620
	40	5.8	11.56	1.94261	1.05169	1.052	(0.26, 0.44)	488, 544, 584, 620
	50	5.8	9.1	0.90149	0.47178	0.511	(0.27, 0.44)	488, 544, 584, 620

	60	6	6.417	1.02573	0.5368	0.546	(0.26, 0.44)	488, 544, 584, 620
CPPOM:*x* wt% $NaGd_{0.6}F_4:Tb_{0.4}$@CzPPOA	30	5.2	13	1.37993	0.8666	0.772	(0.26, 0.45)	488, 544, 584, 620
	40	7	10.24	0.43556	0.19538	0.22	(0.26, 0.46)	488, 544, 584, 620
	50	6.5	17.99	0.38109	0.15955	0.177	(0.26, 0.43)	488, 544, 584, 620
	60	6.5	9.567	0.35842	0.17314	0.2	(0.27, 0.45)	488, 544, 584, 620
CzSi:*x* wt% $NaGd_{0.6}F_4:Tb_{0.4}$@CzPPOA	30	7	3.806	0.41859	0.1643	0.2246	(0.26, 0.42)	488, 544, 584, 620
	40	6.1	4.46	0.99037	0.51829	0.52843	(0.25, 0.43)	488, 544, 584, 620
	50	6.1	2.614	0.57561	0.30124	0.30367	(0.27, 0.44)	488, 544, 584, 620
	60	6	6.56	0.93804	0.49091	0.45407	(0.26, 0.43)	488, 544, 584, 620
DPEPO:*x* wt% $NaGd_{0.6}F_4:Tb_{0.4}$@CzPPOA	30	9.4	2.49	0.0058	0.00202	0.00367	(0.29, 0.37)	488, 544, 584, 620
	40	8.5	3.565	0.0104	0.00384	0.00645	(0.29, 0.37)	488, 544, 584, 620
	50	8.5	2.744	0.02044	0.00755	0.01278	(0.29, 0.37)	488, 544, 584, 620
	60	9	0.9807	0.0071	0.00248	0.00458	(0.30, 0.39)	488, 544, 584, 620
PVK:*x* wt% $NaGd_{0.6}F_4:Tb_{0.4}$@CzPPOA	30	9	31.21	0.40403	0.11533	0.198	(0.29, 0.43)	488, 544, 584, 620
	40	7	21.73	0.89715	0.35213	0.44	(0.28, 0.43)	488, 544, 584, 620
	50	6	10.23	0.79811	0.41768	0.402	(0.27, 0.45)	488, 544, 584, 620
	60	5.5	12.23	0.83935	0.47919	0.418	(0.29, 0.46)	488, 544, 584, 620
*m*CP:*x* wt% $NaGd_{0.6}F_4:Tb_{0.4}$@CzPPOA	20	6.3	32.25	1.16718	0.61054	0.68864	(0.40, 0.54)	488, 544, 584, 620
	25	5.6	33.51	9.19179	5.24768	5.46912	(0.28, 0.54)	488, 544, 584, 620
	30	5.5	28.59	2.92708	1.6711	1.5455	(0.30, 0.56)	488, 544, 584, 620
	35	5.5	32.11	3.59719	2.05367	1.98565	(0.31, 0.56)	488, 544, 584, 620
	40	5.5	24.55	2.00282	1.14343	1.01142	(0.29, 0.53)	488, 544, 584, 620
	45	5.5	21.27	0.96765	0.55244	0.48383	(0.30, 0.55)	488, 544, 584, 620
*m*CP:*x* wt% $NaGd_{0.6}F_4:Tb_{0.4}$@TPPOA	20	5.3	13.07	0.85371	0.50578	0.53784	(0.30, 0.48)	488, 544, 584, 620
	30	7	6.451	0.12135	0.07973	0.07159	(0.29, 0.49)	488, 544, 584, 620
*m*CP:*x* wt% $NaGd_{0.6}F_4:Tb_{0.4}$@tBCzPPOA	10	5.8	6.071	1.09083	0.59055	0.76358	(0.31, 0.53)	488, 544, 584, 620
	20	5.2	6.647	1.34356	0.8113	0.67178	(0.30, 0.52)	488, 544, 584, 620
	30	5.1	7.109	2.16972	1.36259	1.08486	(0.31, 0.52)	488, 544, 584, 620
	40	5.6	7.275	1.10888	0.65696	0.55444	(0.30, 0.51)	488, 544, 584, 620
*m*CP:*x* wt% $NaGd_{0.6}F_4:Tb_{0.4}$@DMACPPOA	10	5.5	6.809	0.63774	0.36409	0.31887	(0.30, 0.52)	488, 544, 584, 620
	20	5.6	8.729	1.07829	0.60461	0.53915	(0.30, 0.47)	488, 544, 584, 620

	30	7	3.273	0.58258	0.26133	0.29129	(0.29, 0.51)	488, 544, 584, 620
	40	7.1	6.396	0.50428	0.2262	0.25718	(0.31, 0.48)	488, 544, 584, 620
*m*CP:*x* wt% $NaGd_{0.6}F_4:Tb_{0.4}$@DPACPPOA	10	5.9	7.744	0.66406	0.37912	0.33203	(0.27, 0.44)	488, 544, 584, 620
	20	5.6	5.666	0.4373	0.24966	0.21865	(0.28, 0.46)	488, 544, 584, 620
	30	5.6	3.597	0.31921	0.17899	0.15961	(0.28, 0.49)	488, 544, 584, 620
	40	5.6	4.16	0.22721	0.1274	0.11361	(0.27, 0.47)	488, 544, 584, 620

[a] Turn-on voltage at 1 cd m^{-2}; [b] the maximum luminance; [c] the maximum EL efficiencies.

Supplementary Table S4. EL performance of ITO|PEDOT:PSS (40 nm)|PVK (20 nm)|*m*CP:*x* wt% $Tb(ligand)_3$ (25 nm)|DPEPO (10 nm)|TmPyPB (40 nm)|LiF (1 nm)|Al devices.

Emitter	*x*	V_{on}[a]	L_{max}[b] (cd m^{-2})	η_{max}[c]			CIE (x, y)	λ (nm)
				η_{CE} (cd A^{-1})	η_{PE} (lm W^{-1})	η_{EQE} (%)		
$Tb(TPPOA)_3$	20	8	4.693	0.46985	0.18442	0.26124	(0.24, 0.54)	488, 544, 584, 620
$Tb(CzPPOA)_3$	25	6.6	205	18.70603	9.03645	4.86357	(0.31, 0.58)	488, 544, 584, 620
$Tb(tBCzPPOA)_3$	30	6.5	179.8	15.74121	7.60421	4.25013	(0.31, 0.61)	488, 544, 584, 620
$Tb(DMACPPOA)_3$	20	9.1	70.7	7.22278	2.51995	2.38352	(0.30, 0.57)	488, 544, 584, 620
$Tb(DPACPPOA)_3$	10	7.1	274.4	13.28769	5.96048	3.98631	(0.29, 0.53)	488, 544, 584, 620

[a] Turn-on voltage at 1 cd m^{-2}; [b] the maximum luminance; [c] the maximum EL efficiencies.

References

1. Han, S.; Deng, R.; Gu, Q.; Ni, L.; Huynh, U.; Zhang, J.; Yi, Z.; Zhao, B.; Tamura, H.; Pershin, A.; Xu, H.; Huang, Z.; Ahmad, S.; Abdi-Jalebi, M.; Sadhanala, A.; Tang, M. L.; Bakulin, A.; Beljonne, D.; Liu, X.; Rao, A., Lanthanide-doped inorganic nanoparticles turn molecular triplet excitons bright. *Nature* **2020,** *587* (7835), 594-599.

2. Dong, A.; Ye, X.; Chen, J.; Kang, Y.; Gordon, T.; Kikkawa, J. M.; Murray, C. B., A Generalized Ligand-Exchange Strategy Enabling Sequential Surface Functionalization of Colloidal Nanocrystals. *Journal of the American Chemical Society* **2011,** *133* (4), 998-1006.

3. Melby, L. R.; Rose, N. J.; Abramson, E.; Caris, J. C., Synthesis and Fluorescence of Some Trivalent Lanthanide Complexes. *Journal of the American Chemical Society* **1964,** *86* (23), 5117-5125.